

RESEARCH ARTICLE

OPEN ACCESS

Dy³⁺ doped Lithium Sodium Bismuth Borate Glasses for Yellow Luminescent Photonic Applications

M. Parandamaiah, K. Naveen Kumar, S. Babu, S. Venkatramana Reddy*, Y.C. Ratnakaram

Department of Physics, Sri Venkateswara University, Tirupati-517 502, Andhra Pradesh, INDIA

*Author for Correspondence e-mail: drsreddy123@gmail.com

ABSTRACT

Lithium sodium bismuth borate glasses-doped with trivalent dysprosium (Dy³⁺) ions (LSBiB) have been prepared by conventional melt-quenching technique and characterized by structural, thermal and spectroscopic measurements. XRD pattern of the host glass confirms its amorphous nature. Morphological and elemental analysis has also been carried out for Dy³⁺-doped LSBiB glass matrix. FTIR spectral analysis confirms the glass formation of the host glass. Optical absorption spectral analysis has been carried out for 0.8 mol% Dy³⁺ doped LSBiB glass sample. Well defined optical absorption bands are assigned with corresponding electronic transitions. Photoluminescence spectra shows two prominent emission bands centered at 482 nm and 575 nm corresponds to the $^4F_{9/2} \rightarrow ^6H_{15/2}$ and $^4F_{9/2} \rightarrow ^6H_{13/2}$ respectively under the excitation of 452 nm. Among all the concentrations of Dy³⁺ ions, at 0.8 mol% Dy³⁺ contained glass sample exhibits prominent yellow emission at 575 nm. Lifetime decay dynamics have been systematically analyzed for all the glasses, higher lifetime is found to be 0.47 ms for 0.8 mol% Dy³⁺ ions doped glass. From the photoluminescence analysis, Dy³⁺ contained glass samples could be suggested as potential yellow luminescent glass matrix for several photonic device applications.

Keywords - Lithium borate glasses- Dy³⁺- Photoluminescence- analysis.

I. INTRODUCTION

In recent years, a special attention has been focused on the rare earth ions doped glasses due to their wide variety of applications in various fields such as solid state lasers, flat panel displays, planar waveguide, optoelectronic devices such as short wavelength (visible) lasers, display devices, sensors and high density frequency domain optical data storage [1]. Among various glasses, borate glasses are excellent host matrices because boric oxide (B₂O₃) acts as a good glass former and flux material [2]. Borate glasses are structurally more intricate as compared to silicate or phosphate glasses due to two types of coordination of boron atoms with oxygens (3 and 4) and the structure of vitreous B₂O₃ consists of a random network of boroxyl rings and BO₃ triangles connected by B-O-B linkages. Moreover, the addition of a modifier oxide causes a progressive change of some BO₃ triangles to BO₄ tetrahedra and results in the formation of various cyclic units like diborate, triborate, tetraborate or pentaborate groups [3]. The glass containing heavy metal ions like Bi₂O₃, PbO, PbF₃, etc., borate glasses, decreases the host phonon energy and thereby improves the effective fluorescence [4] and also the addition of alkali fluoride (NaF) minimizes the phonon energy of the host glass matrix [5]. Moreover, bismuth oxide contained host glass matrix improves chemical durability of the glass [6]. Despite, the Bi₂O₃ is not a

classical network former; it exhibits some superior physical properties like high density, high refractive index and exhibits high optical basicity, large polarizability and large nonlinear optical susceptibility [7]. The presence of two network forming oxides such as classical B₂O₃ and the conditional Bi₂O₃ glass former, the possible participation in the glass structure of both boron and bismuth ions with more than one stable coordination, the capability of the bismuth polyhedral and of the borate structural groups to form independent interconnected networks [8]. Many researchers have well known that the lithium is mor electropositive ion. With the addition of lithium to the borate system, it causes drastic changes in binary lithium borate glass system. Hence, lithium glass forming ability over wide range of composition, higher bond strength, high transparency, low melting point and good rare earth ion solubility. Moreover, lithium borate glasses are useful for solid state battery applications [9, 10]. The luminescence of rare earth doped materials is due to the 4f-4f transitions. This luminescence is due to the shielding effect of the outer orbitals (5s and 5p) on the 4f electrons and it results sharp absorption and emission spectral peaks may be observed [11].

Among the various rare earth ions, Dy³⁺ ion is one of the good luminescent ion which emits blue and yellow and moderate red emission. Despite,

possible visible emission is exhibited from the Dy^{3+} ion, a special attention has also been focused on Dy^{3+} doped complexed materials due its capability of white light emission under the ultraviolet or blue excitation wavelengths [12]. Moreover, Dy^{3+} doped glasses are also used as promising materials for telecommunication technological applications due to their infrared emission at $1.32\text{ }\mu\text{m}$ apart from the display device applications [13]. In our present investigation, the concentration dependent luminescence properties of the Dy^{3+} doped lithium sodium bismuth borate glasses have been systematically analyzed. The structural, morphological, compositional analysis of the host glass and optical absorption, photoluminescence properties of the Dy^{3+} doped glasses are clearly demonstrated.

II. EXPERIMENTAL STUDIES

2.1 Glass samples preparation

The host and Dy^{3+} doped lithium sodium bismuth borate (LSBiB) glass samples with compositions, $(60-x)\text{ B}_2\text{O}_3 + 20\text{LiF} + 10\text{NaF} + 10\text{Bi}_2\text{O}_3 + x\text{Dy}_2\text{O}_3$ (where $x=0.2\text{ mol.\%}, 0.4\text{ mol.\%}, 0.6\text{ mol.\%}, 0.8\text{ mol.\%}, 1.0\text{ mol.\%}, 1.5\text{ mol.\%}$ and 2.0 mol.\% referred to as LSBiBDy0.2, LSBiBDy0.4, LSBiBDy0.6, LSBiBDy0.8, LSBiBDy1.0, LSBiBDy1.5 and LSBiBDy2.0 glasses respectively) were prepared by conventional melt quenching method using high purity precursor chemicals of boric acid (H_3BO_3), bismuth oxide (Bi_2O_3), lithium fluoride (LiF), sodium fluoride (NaF) and dysprosium oxide (Dy_2O_3) powders. About 10g batches of chemicals were mixed and ground using agate mortar to attain homogeneous mixture. The mixture was taken into porcelain crucible and put into electric furnace at a temperature range of $1050\text{--}1100\text{ }^{\circ}\text{C}$ for 45 min. Then the mixture was melted and air quenched by pouring it on a preheated brass plate. These samples were annealed at $300\text{ }^{\circ}\text{C}$ for 3 h in order to remove strains. The density of glass samples was measured using Archimedes principle with xylene as an immersion liquid. The refractive indices were measured at 589.3 nm (sodium wavelength) using an Abbe refractometer with monobromonaphthalene as the contact liquid. For all the glass samples, the physical parameters like density, thickness, refractive index have been calculated.

2.2 Measurements

The XRD spectral profiles of prepared glassy samples were obtained using SEIFERT 303 TT X-ray diffractometer with CuK_{α} (line of 1.5405 \AA), and it was operated at 40 KV voltage and 50 mA anode current. The FTIR spectrum of glass matrix was recorded using Thermo Nicolet IR200 spectrometer at room temperature (RT) in the wavenumber range

of $3000\text{--}400\text{ cm}^{-1}$. Scanning electron microscopy (SEM-CARL ZEISS EVO MA 15) attached with EDAX setup has been employed to investigate the morphological studies and elemental analysis of the prepared glass samples. Optical absorption spectra were recorded using Perkin- Elmer Lambda 950 spectrophotometer in the wavelength range $250\text{--}2500\text{ nm}$. The excitation and visible photoluminescence spectra (range $400\text{--}900\text{ nm}$) and decay spectral profiles of the Dy^{3+} doped glass matrices were recorded using JOBIN YVON Fluorolog-3 fluorimeter using xenon flash lamp.

III. RESULTS AND DISCUSSION

3.1 X-ray diffraction (XRD) analysis

The X-ray diffraction pattern of the Lithium Sodium Bismuth Borate (LSBiB) host glass shows no diffraction peaks were observed, typical long range structural disorder which confirms the amorphous nature of the glass [14]. As the profile was similar in all the eight glasses and the one host glass (LSBiB) is shown in Fig.1.

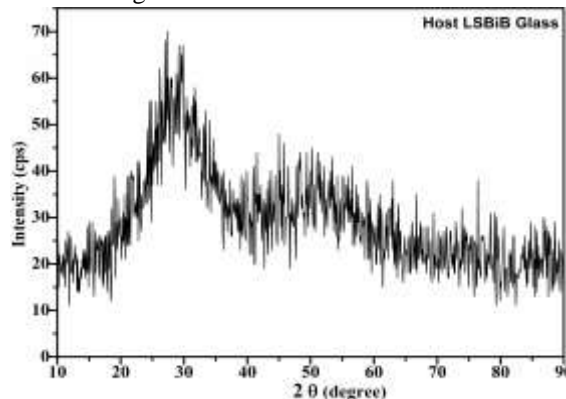


Fig.1 XRD profile of the host $60\text{H}_3\text{BO}_3 + 20\text{LiF} + 10\text{NaF} + 10\text{Bi}_2\text{O}_3$ glass.

3.2 Scanning electron microscopy (SEM) and EDAX studies

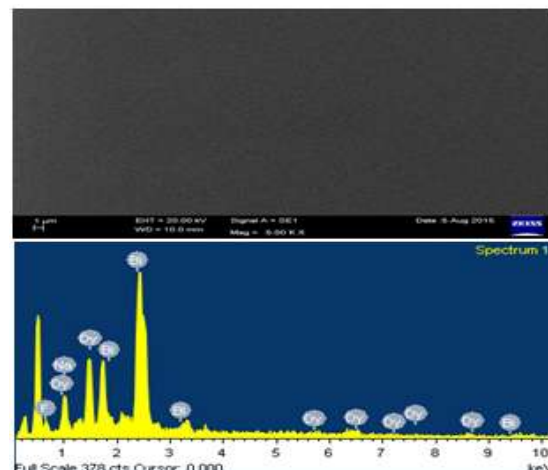


Fig.2 SEM (upper) and EDAX (down) profiles $59.2\text{H}_3\text{BO}_3 + 20\text{LiF} + 10\text{NaF} + 10\text{Bi}_2\text{O}_3 + 0.8\text{ Dy}$ glass samples.

SEM image explores the smooth surface of the sample. This smooth surface indicates that the amorphous behavior of the glass matrix and also we cannot identify any grain boundaries from the surface morphological image of the host LSBiB glass sample as shown in **Fig. 2 (a)**. The elemental analysis has been carried out from the EDAX spectral profile as shown in **Fig. 2 (b)**. The spectrum gives information about the elements which are present in the investigated glass samples.

3.3 FTIR analysis

The FTIR spectrum of host $\text{B}_2\text{O}_3+\text{LiF}+\text{NaF}+\text{Bi}_2\text{O}_3$ (LSBiB) glass is shown in **Fig.3**. The spectrum revealed that the characteristic peaks are located at 516 cm^{-1} , 667 cm^{-1} , 896 cm^{-1} , 1218 cm^{-1} , 1360 cm^{-1} , 1546 cm^{-1} , 1740 cm^{-1} , 2341 cm^{-1} , 3020 cm^{-1} and 3732 cm^{-1} . The broad bands are due to combination of several factors such as high degeneracy of vibrational state, thermal broadening of lattice dispersion and mechanical scattering from the sample. The infrared bands are mainly related to BO_3 and BO_4 groups. The FTIR transmission band in the range of $400-650 \text{ cm}^{-1}$ is assigned to B-O-B bending vibrations as well as borate ring deformation [15].

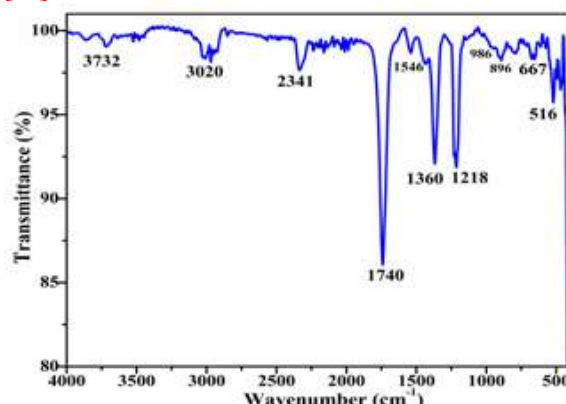


Fig.3 FTIR spectrum of the host $60\text{H}_3\text{BO}_3+20\text{LiF}+10\text{NaF}+10\text{Bi}_2\text{O}_3$ glass.

It can be seen that the band at 667 cm^{-1} is attributed to the bending vibration of the B-O-B linkage in the borate network, which had already reported in the earlier literature [16]. It is also observed that the band observed at $665-714 \text{ cm}^{-1}$ is due to the B-O-B bending vibrations of BO_3 triangles [17]. The band at around 1360 cm^{-1} has been assigned to the stretching of trigonal BO_3 units in meta, ortho and pyro-borate groups [18]. The band centered at 986 cm^{-1} is assigned to B-O stretching vibrations of tetrahedral BO_4 units in different borate groups. The band region from $850-982 \text{ cm}^{-1}$ is related to the symmetrical stretching vibration of BO_4 units. The transmission band at 1218 cm^{-1} is specific principle signature to the B-O stretching vibrations of BO_3 triangular units with non-bridging oxygen atoms

[19]. The FTIR spectral transmission peak observed in the region of $2500-4000 \text{ cm}^{-1}$ is attributed to water groups OH stretching vibrations.

3.4 Optical absorption spectral analysis

Fig. 4 (a & b) shows the optical absorption spectra of both visible and NIR regions of the 0.8 mol% doped LSBiB glass sample recorded at room temperature in the wavelength region of 310-500 nm and 730-1800 nm.

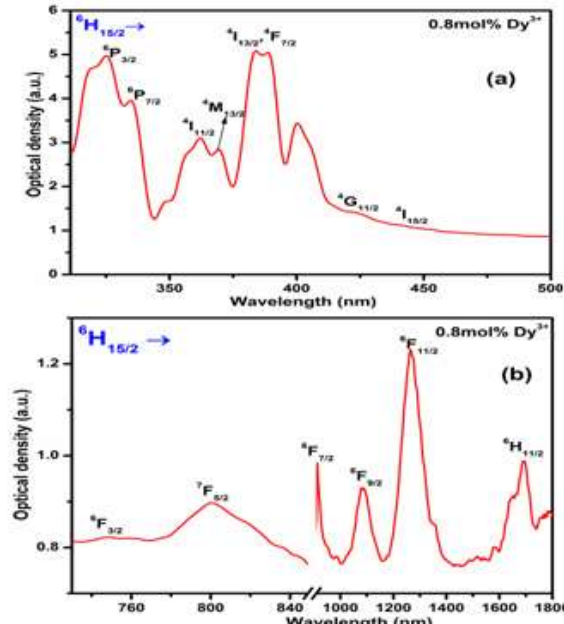


Fig.4 Optical absorption spectrum of the (0.8 mol%) Dy^{3+} : $60\text{H}_3\text{BO}_3+20\text{LiF}+10\text{NaF}+10\text{Bi}_2\text{O}_3$ glass.

Well defined absorption bands pertaining to Dy^{3+} ions corresponding to the transition starting from the $^6\text{H}_{15/2}$ ground state to various excited states. From absorption spectra we have observed the several absorption bands at 324 nm, 335 nm, 362 nm, 369 nm, 384 nm, 423 nm, 442 nm in the UV-Vis region and these absorption peaks are assigned to corresponding electronic transitions as $^6\text{H}_{15/2} \rightarrow ^6\text{P}_{3/2}$, $^6\text{H}_{15/2} \rightarrow ^6\text{P}_{7/2}$, $^6\text{H}_{15/2} \rightarrow ^4\text{I}_{11/2}$, $^6\text{H}_{15/2} \rightarrow ^6\text{M}_{13/2}$, $^6\text{H}_{15/2} \rightarrow ^4\text{I}_{13/2}$, $^4\text{F}_{7/2}$, $^6\text{H}_{15/2} \rightarrow ^4\text{G}_{11/2}$ and $^6\text{H}_{15/2} \rightarrow ^4\text{I}_{15/2}$ respectively [20]. We have observed the absorption bands in the NIR region at 747 nm, 800 nm, 912 nm, 1080 nm, 1272 nm and 1692 nm and these bands are assigned with corresponding electronic transitions as $^6\text{H}_{15/2} \rightarrow ^4\text{F}_{3/2}$, $^6\text{H}_{15/2} \rightarrow ^7\text{F}_{5/2}$, $^6\text{H}_{15/2} \rightarrow ^6\text{F}_{7/2}$, $^6\text{H}_{15/2} \rightarrow ^6\text{F}_{9/2}$, $^6\text{H}_{15/2} \rightarrow ^6\text{F}_{11/2}$ and $^6\text{H}_{15/2} \rightarrow ^6\text{H}_{11/2}$ respectively [21].

3.5 Photoluminescence studies

In order to understand the luminescence properties of LSBiBDy glasses, it is very essential to aware of the suitable excitation wavelengths of Dy^{3+} ions. The excitation spectrum of the Dy^{3+} (0.8%) contained LSBiBDy glass is shown in **Fig. 5**.

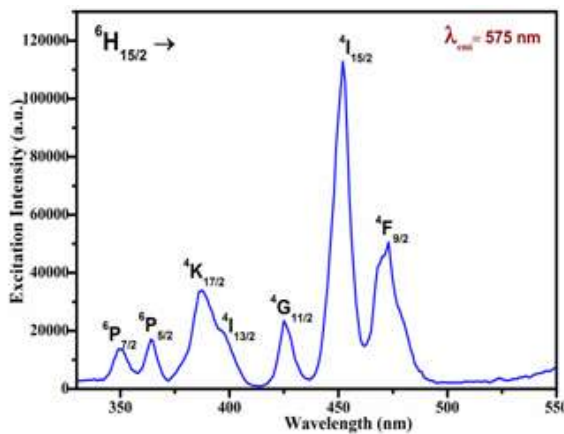


Fig.5 Excitation spectrum of the (0.8 mol %) Dy^{3+} : $60H_3BO_3 + 20LiF + 10NaF + 10Bi_2O_3$ glass.

The excitation spectrum exhibits the seven excitation bands by monitoring an intense emission at 575 nm in the spectral region of 325-550 nm. The excitation bands are observed at 349, 364, 386, 396, 425, 451 and 468 nm and these excitation bands are assigned with corresponding electronic transitions $^6H_{15/2} \rightarrow ^6P_{7/2}$, $^6H_{15/2} \rightarrow ^6P_{5/2}$, $^6H_{15/2} \rightarrow ^4K_{17/2}$, $^6H_{15/2} \rightarrow ^4I_{13/2}$, $^6H_{15/2} \rightarrow ^4G_{11/2}$, $^6H_{15/2} \rightarrow ^4I_{15/2}$ and $^6H_{15/2} \rightarrow ^4F_{9/2}$ respectively [22]. It is well known fact that the intense excitation wavelength can gives the intense emission of the emissive ions. Of all the excitation bands, a band at 452 nm ($^6H_{15/2} \rightarrow ^4I_{15/2}$) shows prominent intensity than the other excitation bands and this preferable wavelength has also been chosen to obtain the emission spectrum.

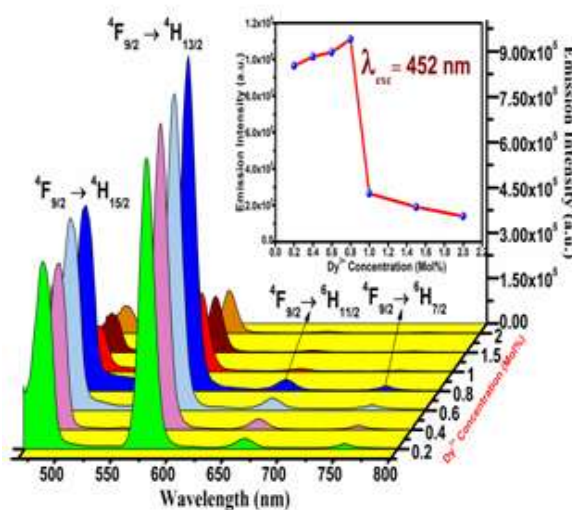


Fig.6 Emission spectra of Dy^{3+} (0.2, 0.4, 0.6, 0.8, 1, 1.5 and 2 mol%): $60H_3BO_3 + 20LiF + 10NaF + 10Bi_2O_3$ glasses under the excitation of 452 nm.

The emission spectra of various concentrations of Dy^{3+} ions doped LSBiB glasses are recorded in the range of 465-800 nm and it is shown in **Fig.6**. Dy^{3+} ions are excited to ($4f^85d$) upper energy level under

an excitation with 452 nm. From these excited ions cascade rapidly towards $^4F_{9/2}$ state through $^4G_{11/2}$, $^4I_{15/2}$ levels and then finally relaxes non-radiatively by populating $^4F_{9/2}$ meta-stable state. The non-radiative decay is very fast because of closely spaced $4f^9$ levels between $^4F_{9/2}$ and $4f^85d$ levels. On reaching $^4F_{9/2}$ level, these unstable ions relax radiatively by emitting fluorescence to the nearest lower lying multiplet 6H_J ($J=15/2$, $13/2$, and $11/2$) energy level [23].

The emission spectra exhibit two major emission bands at 482 nm and 575 nm in blue and yellow regions. Along with these two bands, another two low intense bands have also been observed at 660 nm and 752 nm. These emission bands are assigned with corresponding electronic transitions as 482 nm ($^4F_{9/2} \rightarrow ^6H_{15/2}$), 575 nm ($^4F_{9/2} \rightarrow ^6H_{13/2}$), 660 nm ($^4F_{9/2} \rightarrow ^6H_{11/2}$) and 752 nm ($^4F_{9/2} \rightarrow ^6H_{7/2}$). The prominent emission transition $^4F_{9/2} \rightarrow ^6H_{13/2}$ is hypersensitive electric – dipole transition with $\Delta J = \pm 2$ and $\Delta L = \pm 2$, which has been strongly influenced by the local coordination environment. Another intense emission transition $^4F_{9/2} \rightarrow ^6H_{15/2}$ is a magnetic-dipole transition with $\Delta J = 0, \pm 1$ and less sensitive to the local coordination environment. From the emission spectral profile, $^4F_{9/2} \rightarrow ^6H_{13/2}$ transition exhibits the predominant intensity than $^4F_{9/2} \rightarrow ^6H_{15/2}$ transition. The analysis of yellow-to-blue luminescence intensity ratio (Y/B) is used to characterize the Dy^{3+} - O^{2-} bond covalence and the higher value of the Y/B indicates the higher degree of covalency between Dy^{3+} and O^{2-} ions [24]. Upon increasing the concentration of Dy^{3+} ions from 0.2 to 0.8 mol % in the LSBiB glass system, the yellow emission intensity is significantly enhanced as shown in **Fig. 6**. Nevertheless, the drastic decrement in the emission intensity values has observed at higher concentration of the Dy^{3+} ions (above 0.8 mol %) in the LSBiB glass matrix as shown in inset of **Fig. 6**. This could be due to concentration quenching effect [25]. The concentration quenching is quite related to the higher concentrations of mutual Dy^{3+} - Dy^{3+} interactions. The huge amount of non-radiative energy transfer through cross relaxation and resonant energy channels is also influenced the concentration quenching. This is in good agreement with the earlier report [26].

The energy level scheme diagram of the Dy^{3+} ions emission analysis has clearly demonstrated in the **Fig. 7**.

3.6 Lifetime Decay analyses

The fluorescence decay curves of $^4F_{9/2}$ state of Dy^{3+} doped LSBiB glasses are obtained at 452 nm and monitoring the emission at 575 nm at room temperature. The decay curves are shown in **Fig. 8**.

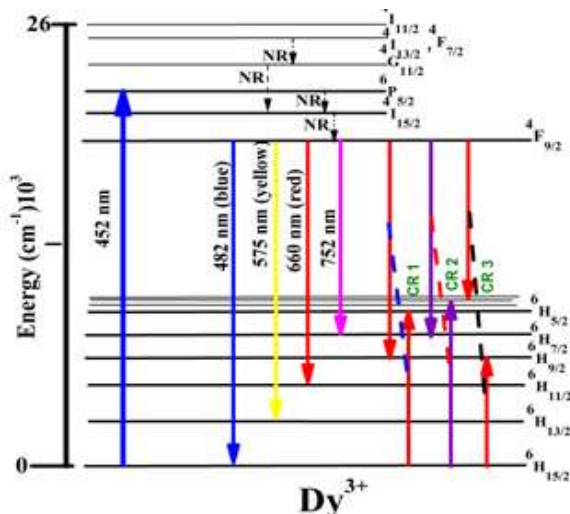


Fig. 7 Schematic energy level diagram of Dy^{3+} doped LSBiB glasses.

The fluorescence decay curves are well fitted to nearly single exponential up to 0.8 mol% of Dy^{3+} ions concentration in accordance with the first order decay behavior as

$$I_t = I_0 \exp(-t / \tau) \quad \text{--- (1),}$$

where I_t and I_0 is the intensity at time t and 0, and τ is defined as the luminescent lifetime. Above 0.8 mol%, it exhibits non-exponential behavior as per the below equation,

$$I(t) = A_1 \exp(-t / \tau_1) + A_2 \exp(-t / \tau_2) \quad \text{--- (2),}$$

where $I(t)$ is the emission intensity, A_1 and A_2 are constants, τ_1 and τ_2 are the short and long lifetimes for the exponential components, respectively. The average life time (τ_{avg}) of $^4F_{9/2}$ level has been determined by the formula [27] as given below

$$\tau_{avg} = \frac{A_1 \tau_1^2 + A_2 \tau_2^2}{A_1 \tau_1 + A_2 \tau_2} \quad \text{--- (3)}$$

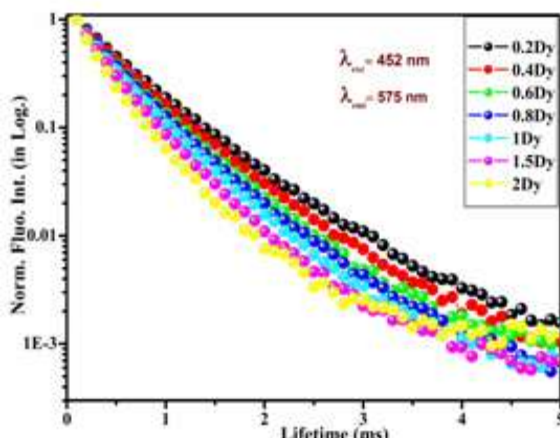


Fig. 8. Lifetime of the Dy^{3+} (0.2, 0.4, 0.6, 0.8, 1, 1.5 and 2 mol%) : $60H_3BO_3+20LiF+10NaF+10Bi_2O_3$ glasses using 452 nm excitation and 575 nm emission.

From the decay analysis, lifetime values have been mentioned in the Table 1. The higher life time value is found to be 0.47 ms for 0.8 mol% Dy^{3+} doped LSBiB glass sample than the other concentrations of Dy^{3+} doped glasses.

IV. Conclusions

In summary, it could be concluded that the optical glasses of $(60-x) B_2O_3 + 20LiF+10NaF+10Bi_2O_3 + xDy_2O_3$ (where $x=0.2$ mol.%, 0.4 mol.%, 0.6 mol.%, 0.8 mol.%, 1.0 mol.%, 1.5 mol.% and 2.0 mol.%) have been synthesized by melt quenching method. The structural, morphological and compositional analysis of host glass has been demonstrated by XRD, SEM and FTIR studies. Optical absorption bands have been assigned with corresponding electronic transitions in absorption spectrum of Dy^{3+} (0.8 mol %) doped glass. From the photoluminescence studies, Dy^{3+} doped glasses exhibit a strong yellow emission at 575 nm and moderate intense blue emission at 482 nm which are assigned with corresponding electronic transitions of $^4F_{9/2} \rightarrow ^6H_{13/2}$ and $^4F_{9/2} \rightarrow ^6H_{15/2}$ respectively under the excitation of 452 nm. Among all the Dy^{3+} doped glasses at different concentrations of the Dy^{3+} ions, 0.8 mol% Dy^{3+} doped glass has shown an intense yellow emission at 575 nm. The optimized concentration of the Dy^{3+} ion has been found to be 0.8 mol% based on the photoluminescence performances. The lifetime decay dynamics have also been systematically demonstrated. These optical glasses doped with Dy^{3+} ions could be suggested as promising materials for yellow luminescent photonic devices.

REFERENCES

- [1] D. Rajesh, A. Balakrishna, Y.C. Ratnakaram, *Luminescence, structural and dielectric properties of Sm^{3+} impurities in strontium lithium bismuth borate glasses*. Opt. Mat. **35** (2012) 108–116.
- [2] M. Subhadra, P. Kistaiah, *Infrared and raman spectroscopic studies of alkali bismuth borate glasses: Evidence of mixed alkali effect*, Vibrational Spectroscopy **62** (2012) 23–27.
- [3] D.D. Ramteke, K. Annapurna, V.K. Deshpande, R.S. Gedam, *Effect of Nd^{3+} on spectroscopic properties of lithium borate glasses*, J. Rare Earths **32**(12) (2014) 1148–1153.
- [4] P. Srivastava, S. B. Rai, D. K. Rai, *Optical properties of Dy^{3+} doped calibo glass on addition of lead oxide*, Spectrochim. Acta A **59** (2003) 3303–3311.
- [5] P. Pascuta, L. Pop, S. Rada, M. Bosca, E. Culea, *The local structure of bismuth borate glasses doped with europium ions evidenced*

- by FT-IR spectroscopy, J. Mater. Sci.: Mater. Electron. **19** (2008) 424-428.
- [6] J.L. Doualan, S. Girard, H. Haquin, J.L. Adam, J. Montagne, Spectroscopic properties and laser emission of Tm doped ZBLAN glass at 1.8 μm , Opt. Mat. **24** (2003) 563–577.
- [7] S.P. Singh, R.P.S. Chakradhar, J.L. Rao, B. Karmakar, EPR, optical absorption and photoluminescence properties of MnO_2 doped $23\text{B}_2\text{O}_3\text{-}5\text{ZnO}\text{-}72\text{Bi}_2\text{O}_3$ glasses, Phys. B **405** (2010) 2157-2161.
- [8] P. Pascuta, G. Borodi, E. Culea, Influence of europium ions on structure and crystallization properties of bismuth borate glasses and glass ceramics, J. Non-Cryst. Solids **354** (2008) 5475- 5479.
- [9] R. S. Gedam, D. D. Ramteke, Electrical and optical properties of lithium borate glasses doped with Nd_2O_3 , J. Rare Earths **30** (8) (2012) 785-789.
- [10] R. S. Gedam, D. D. Ramteke, Influence of CeO_2 addition on the electrical and optical properties of lithium borate glasses, J. Phys. Chem. Solids **74** (2013) 1399-1402.
- [11] G. Lakshminarayana, J. Qiu, M. G. Brik, I. V. Kityk, Photoluminescence of Eu^{3+} -, Tb^{3+} -, Dy^{3+} - and Tm^{3+} -doped transparent $\text{GeO}_2\text{-TiO}_2\text{-K}_2\text{O}$ glass ceramics, J. Physics: Condens. Matter **20**(33) (2008) 335106.
- [12] Zhongfei Mu, Yihua Hu, Li Chen , Xiaojuan Wang, Enhanced luminescence of Dy^{3+} in $\text{Y}_3\text{Al}_5\text{O}_{12}$ by Bi^{3+} co-doping, J. Lumin. **131** (2011) 1687-1691.
- [13] Z. Duan, J. Zhang, L. Hu, Spectroscopic properties and Judd-Ofelt theory analysis of Dy^{3+} doped oxyfluoride silicate glass, J. Appl. Phys. **101** (2007) 043110–043116.
- [14] Yasser SalehMustafaAlajerami, Suhairul Hashim, Wan Muhamad SaridanWan Hassan, Ahmad Termizi Ramli, Azman Kasim, Optical properties of lithium magnesium borate glasses doped with Dy^{3+} and Sm^{3+} ions, Physica B **407** (2012) 2398–2403.
- [15] N. A. El-Alaily, R. M. Mohamed, Effect of irradiation on some optical properties and density of lithium borate glass, Mat. Sci. Eng. B **98** (2003) 193–203.
- [16] Chandrikam Gautam, Avadhesh Kumar Yadav, Arbind Kumar Singh, A Review on Infrared Spectroscopy of Borate Glasses with Effects of Different Additives, ISRN Ceramics Article ID **428497** (2012) 1-17.
- [17] Safeya Ibrahim, Mohamed Mahmoud Gomaa, Hussein Darwish, Influence of Fe_2O_3 on the physical, structural and electrical properties of sodium lead borate glasses, J. Adv. Ceram. **3**(2) (2014) 155-164.
- [18] Vandana Sharma, Supreet Pal Singh, Gurmel Singh Mudahar, Kulwant Singh Thind, Synthesis and Characterization of Cadmium Containing Sodium Borate Glasses, New J. Glass Ceram. **2** (2012) 150-155.
- [19] V. Simon, M. Spinu, R. Stefan, Structure and dissolution investigation of calcium-bismuth- borate glasses and vitroceramics containing silver, J. Mater Sci: Mater Med **18** (2007) 507-512.
- [20] A.M. Babu, B.C. Jamalaiah, J. S. Kumar, T. Sasikala, L. R. Moorthy, Spectroscopic and photoluminescence properties of Dy^{3+} -doped lead tungsten tellurite glasses for laser materials, J. Alloys Compd. **509** (2011) 457-462.
- [21] Ying Tian, Rongrong Xu, Lili Hu, Junjie Zhang, Broadband 2.84 μm luminescence properties and Judd-Ofelt analysis in Dy^{3+} -doped $\text{ZrF}_4\text{-BaF}_2\text{-LaF}_3\text{-AlF}_3\text{-YF}_3$ glass, J. Lumin. **132** (2012) 128-131.
- [22] M. V Vijaya Kumar, B. C. Jamalaiah, K. Rama Gopal, R. R. Reddy, Optical absorption and fluorescence studies of Dy^{3+} -doped lead telluroborate glasses, J. Lumin. **132** (2012) 86-90.
- [23] I. Pekgozlu, S. Cakar, Photoluminescence properties of $\text{Li}_6\text{CaB}_3\text{O}_{8.5}$: M^{3+} (M^{3+} : Dy and Sm), J. Lumin. **132** (2012) 2312-2317.
- [24] I. M. Nagpure, V. B. Pawade, S. J. Dhoble, Combustion synthesis of $\text{Na}_2\text{Sr}(\text{PO}_4)\text{F}:\text{Dy}^{3+}$ white light emitting phosphor, J. Lumin. **25** (2010) 9-13.
- [25] D. Rajesh, Y. C. Ratnakaram, M. Seshadri, A. Balakrishna, T. Satya Krishna, Structural and luminescence properties of Dy^{3+} ion in strontium lithium bismuth borate glasses, J. Lumin. **132** (2012) 841-849.
- [26] S. A. Azizan, S. Hashim, N. A. Razak, M. H. A. Mharedb, Y.S. M. Alajerami, N. Tamchek, Physical and optical properties of Dy^{3+} : $\text{Li}_2\text{O}\text{-K}_2\text{O}\text{-B}_2\text{O}_3$ glasses, J. Mol. Structure **1076** (2014) 20-25.
- [27] R. Vijayakumar, G.Venkataiah, K. Marimuthu, White light simulation and luminescence studies on Dy^{3+} doped Zinc borophosphate glasses, Physica B **457**(2015)287–295.